# First Principles Simulation of Grain Boundary Sliding

C. Molteni, G. P. Francis, M. C. Payne, and V. Heine
*Theory of Condensed Matter, Cavendish Laboratory, University of Cambridge,*
*Madingley Road, Cambridge CB3 OHE, United Kingdom*

(Received 19 September 1995)

We present the results of a total-energy pseudopotential simulation of the sliding process at a $\Sigma = 5$ (001) twist grain boundary in germanium. Sliding involves a stick-slip mechanism with local rebonding among a few atoms, accompanied by the clearance of gap states. At large strain, spreading of disorder from the boundary interface produces a loss of strength in the system and would induce fracture. Finally we investigate the effects of temperature and strain rate on the sliding behavior.

PACS numbers: 61.72.Mm, 62.20.Fe, 71.10.–w

Grain boundary sliding (i.e., the sliding of one grain over another parallel to the boundary interface that occurs in response to applied forces) plays an important role in the deformation and fracture processes of polycrystalline materials, particularly at high temperature [1]. We report here the first *ab initio* simulation of the sliding at a semiconductor grain boundary, designed to elucidate the evolution of the atomic configuration around the interface. Our computer experiment consists of the sliding at a $\Sigma = 5$ (001) twist grain boundary in germanium, this being chosen as a typical covalently bonded material. The simulation run is analyzed in detail to show the atomistic processes associated with the sliding at the boundary. More generally, our investigation addresses the bond breaking and remaking mechanisms that occur in a semiconductor in response to applied deformation forces or in thermally activated processes.

The $\Sigma = 5$ (001) twist boundary may be ideally formed by bringing together the (001) faces of two diamond cubic semicrystals and rotating one grain with respect to the other by 36.9° about the [001] axis. The structure has a superperiodicity, the coincidence site lattice (CSL), defined by the atoms (1 out of 5) shared by the two grains, and has previously been investigated with pseudopotential density functional techniques [4]. The above construction does not yield a unique boundary structure because one grain may still be translated rigidly with respect to the other by any amount within the irreproducible zone of the displacement shift complete lattice (DSCL) unit cell [5]. Earlier analysis [2–4] showed that many relaxed structures of the Ge $\Sigma = 5$ (001) twist boundary can be obtained, all with similar energies in the range $1.18-1.44\ \mathrm{J\,m^{-2}}$: This effect is due to the inherent frustration between the imposed twist geometry and the tendency to form bonds in specific directions. Indeed, the discovery of the complexity of the grain boundary structure motivated the present study since the previous results gave no indication of how the structure of the boundary would change under continuous deformation.

In our simulation, two slablike grains, consisting of 6 and 8 germanium layers of 5 atoms each, with two equivalent twist boundaries between them, are modeled in a periodically repeated orthorhombic cell of dimensions $a_1 = \sqrt{10}\,a/2$, $a_2 = \sqrt{10}\,a/2$, and $a_3 = 7a/2$, where $a$ is the cubic lattice constant of Ge, along the $[-130]$, [310], and [001] directions, respectively. $a_1$ and $a_2$ are the CSL base vectors, and $a_3$ was initially adjusted in order to take into account the volume expansion at the boundary in the [001] direction [4]. The four layers that enclose each boundary are free to relax, the others being kept frozen in their bulk positions. Since the presence of the grain boundary affects just a very narrow region around the interface [6], the chosen separation is sufficient to avoid significant artificial interactions.

The simulation consists of total-energy calculations within the density functional theory in the local density approximation. We use a local pseudopotential for the germanium ion cores [4], a plane wave basis for the electron wave functions with a cutoff energy of 125 eV, and the conjugate gradient minimization technique [7]. Two special $\mathbf{k}$ points at (1/4, 1/4, 0) and (−1/4, 1/4, 0) are used for the integration over the Brillouin zone. The reliability of these simulation parameters has been established in Ref. [4].

The sliding process has been simulated quasistatically in a sequence of 100 steps, each consisting of a rigid shift of one grain with respect to the other of 1/100 of the CSL cell face diagonal. The ionic positions are then relaxed to equilibrium. During the sliding the volume of the simulation cell has been kept fixed, but we have monitored the stress at each step and found no appreciable changes. Hence, this constraint is not believed to have a significant effect on our simulation. In any case, simulation at constant $a_3$ corresponds very closely to sliding at a large area grain boundary made up of a patchwork of different low-energy structures. The initial boundary configuration [which corresponds to a translational state of $(-1/20a_1, 1/20a_2, 0)$ and is shown in Fig. 1] is the one, among those investigated previously [4], with both lower energy and the best bonding, having most atoms in fourfold coordination. This boundary is characterized by in-plane bonds which we call dimers by analogy with the (100) surface.

0031-9007/96/76(8)/1284(4)$06.00

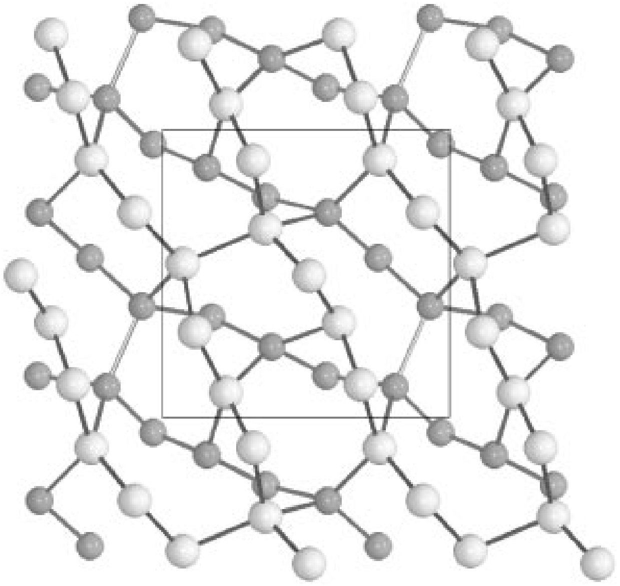

FIG. 1. The initial structure of the Ge $\Sigma = 5(001)$ twist grain boundary. Two layers above (light atoms) and two layers below (dark atoms) the boundary plane are shown. The CSL cell is represented.

The evolution of the grain boundary energy during the sliding (Fig. 2) shows a recurrent pattern of stick–slip events. In these the energy increases quasielastically and then it drops suddenly. The energy jumps correspond to rebonding processes that occur when the stress (given by the slope of the energy curve in Fig. 2) becomes too high.

By comparing the atomic positions before and after each energy jump, we have found that the change in the bonding topology is always localized on a small cluster of atoms, e.g. that shown in Fig. 3 for the case of the first energy jump. The dimers originally present in the boundary remain strongly bonded in spite of the fact that they are starting to cause a substantial local strain, while two new dimers form, one above the other (Fig. 3, right), giving rise to two adjacent sixfolded rings.

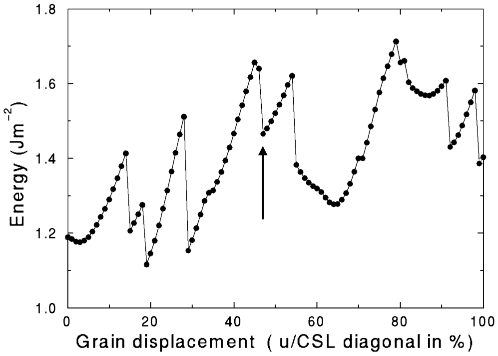

FIG. 2. The grain boundary energy during the sliding process. The arrow shows where disorder starts to migrate away from the boundary interface.

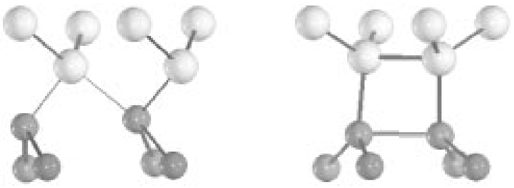

FIG. 3. The structure of the group of atoms that modify their positions significantly before (left) and after (right) the first energy jump. The two shades (light and dark) distinguish the atoms at opposite sides of the boundary.

Initially, the rebonding processes produce low energy configurations with internal shear stresses similar to those before the energy jump; the strengths of the new structures are all comparable with that of the starting configuration, and in this regime the system is capable of resisting any further deformation. However, this behavior eventually changes; the new configurations after the jumps have higher energies and smaller, in some cases negative, stress. These higher energy structures show some plastic deformation: beyond the point indicated by the arrow in Fig. 2, disorder ceases to be confined within the two layers that border the boundary interface, and the bond breaking spreads to bonds between the second and the third layer away from the boundary. The mean stress also decreases, indicating the weakening of the boundary that ultimately results in fracture.

Our simulation throws light on another matter. It is part of the folklore of semiconductor physics that states in the gap extracted from the valence band increase the total energy, so that movements toward low-energy structures will be accompanied by a reduction in the number of gap states or even in their total elimination. We have found that indeed the number of gap states is greatly reduced at each energy jump, as shown in Fig. 4, where the densities of states near the band gap before and after the third energy jump are shown. The densities of states have been

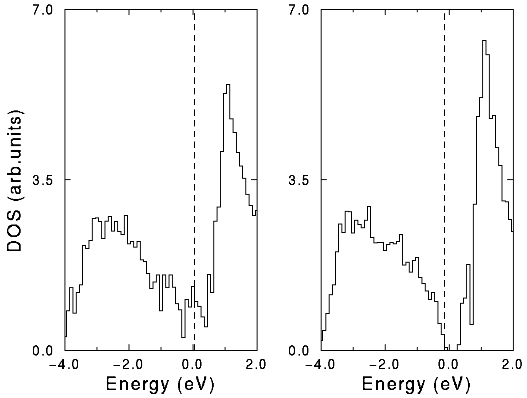

FIG. 4. The electronic density of states of the grain boundary near the band gap before (left) and after (right) the third energy jump. The dashed lines indicate the Fermi level.

calculated for the atomic configurations from the *ab initio* simulation, using a tight–binding model, with a $sp^3s^*$ basis set [8], which gives a good band structure for Ge, with a fully converged integration over the Brillouin zone. Note that the gap states are not wholly eliminated; this may have consequences for pinning of the Fermi level and for the electrical properties.

Since grain boundary sliding is significant mainly at fairly high temperatures ($T > 0.4T_{\mathrm{melt}}$ [1]) and our simulation has been carried out at zero temperature, we have developed a qualitative picture of thermal effects on the sliding behavior. By running the simulation backwards from points after the first, second, and third energy jumps, respectively, we have completed the elastic energy curves associated with the first three rebonded configurations: The resulting curves are shown in Fig. 5. We define the intersections of the forward and backward energy curves as *crossovers*. The topology of the bond structure does not change along each elastic curve, although differences in the bond lengths and bond angles, due to the increasing strain, can be observed. The structural transformations to pass from one curve to the other are basically the same at the crossovers, at the jump points, and for shear displacements in between. As previously discussed, at zero temperature the rebonding processes occur spontaneously only at the jump points, when the system has become unstable because of the high built-in internal stress. On the contrary, at finite temperature the system can undergo a structural transformation to pass from one curve to the other either spontaneously at the jump points, or at lower value of the relative grain displacement $u$, where it is still in a metastable state, provided it has enough energy to overcome the energy barrier $E_b(u)$ associated with the structural transformation involved. In this last case the process has to be thermally activated. At high temperature the system should be able to overcome the barriers at the crossovers and hence to follow the lower energy path highlighted by the filled symbols in Fig. 5, without passing through configurations of high internal stress. The barriers $E_b$ at the first three crossovers have been found to be 0.10, 0.52, and 0.67 eV, respectively, considerably below the activation energy for bulk self–diffusion (3.14 eV) [9].

The rebonding transformation that occurs at II has been investigated in great detail: In essence, it consists of the rotation of a single bond connecting two atoms on opposite sites of the boundary, through an angle of about 80°. This process resembles the first half of the concerted exchange mechanism proposed for self–diffusion in Si [10]. Thus we can consider the angle of rotation $\theta$ that the bond makes with its original direction as a single transformation coordinate. The energy barrier function $E(\theta, u)$ has been determined from the calculation of the total energy of the system at fixed grain displacement $u$, at constrained values of $\theta$ between zero and its final value $\theta_f$, fixing the center of the bond but relaxing all the other ionic degrees of freedom. The barrier height $E_b(u)$ is the maximum value of $E(\theta, u)$ above the initial energy $E(0, u)$. The results are shown in Fig. 6. We find, as expected, that $E_b(u)$ decreases monotonically to zero at the instability point ($u = u_J = 19\%$, where the jump occurs in our $T = 0$ K simulation in Fig. 5). We can now study the mechanism to jump from one curve to the other, assuming for simplicity that only the configurations on the two curves that cross at II are involved in the process. Let us consider the system initially at some $u_0$ before II on the lower energy curve (e.g. $u_0 = 6\%$), with a grain sliding velocity $v$, representing the strain rate. The rate of overcoming the barrier when the system is on the initial curve is $\kappa(t;\, T;\, v) = \nu \exp[-E_b(u)/K_B T]$, where as a first approximation we take $\nu$ as the TO($\Gamma$) phonon frequency and $u = u_0 + vt$. The probability $\mathcal{P}(t; T; v)$ of having made the jump, taking into account both forward and backward jumps between the two curves, is then calculated. We can thus characterize the rebonding process by the time $t_R$ when $\mathcal{P}$ reaches $1/2$ and by the corresponding point $u_R = u_0 + vt_R$ where rebonding has occurred. The results (Fig. 7) show, as expected,

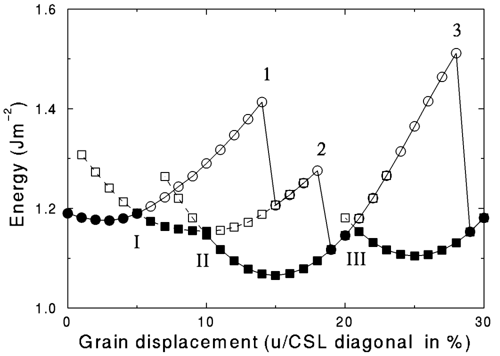

FIG. 5. The grain boundary energy for forward (circles) and backward (squares) applied strain. The filled symbols highlight the high temperature energy path.

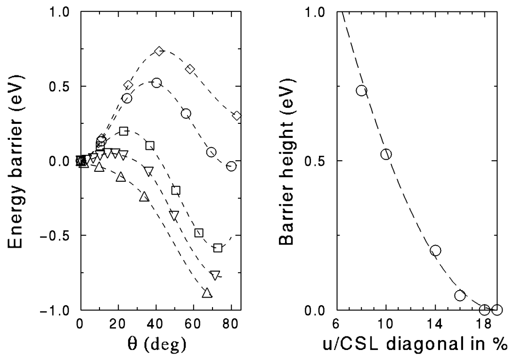

FIG. 6. The energy barriers (left) for the structural transformation associated with the II crossover at different values of the grain displacement $u$: $u$ equal to 8% (diamonds), 10% (circles), 14% (squares), 16% (triangles down), and 18% (triangles up). The right panel shows the corresponding barrier heights.

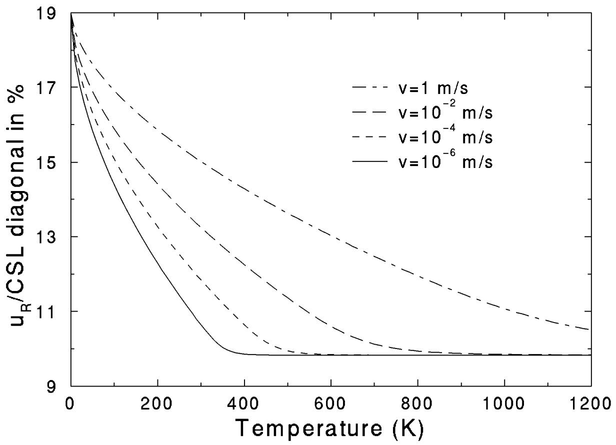

FIG. 7. The rebonding relative grain displacement as a function of temperature for different sliding velocities.

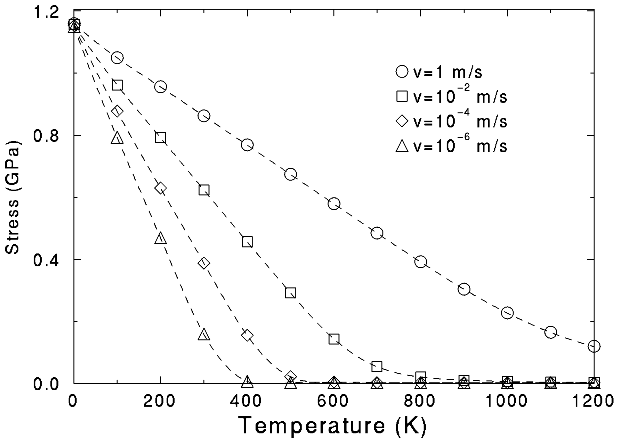

FIG. 8. The average excess stress as a function of temperature for different sliding velocities.

that at high temperature or slow velocity the rebonding occurs near the crossover, whereas at low $T$ or high $v$ it occurs at larger $u$ with limiting value $u_J$ (the jump in Fig. 5). Finally, we can estimate the average stress as a function of temperature and sliding velocity by summing the probabilities of being on the upper and lower curves multiplied by the respective stresses and then averaging over $u$. The difference between the calculated average stress between $u_0$ and $u_J$ when the system rebonds at $u_R$ and the average stress that the system would have following the lower energy path in Fig. 5 is shown in Fig. 8. This gives an estimate of the stress needed for the sliding. In fact if we imagine the real system made by a patchwork of different low-energy structures [4], following completely the lower energy curves such as the one in Fig. 5, as it would at high temperature, then the mean stress over many rebonding events would be zero. It is therefore reasonable to assume the average stress over the lower energy curve as the reference stress.

Hence we propose the following qualitative picture: At very low temperatures the rebonding processes can only occur at the spontaneous jump points as originally calculated, whereas at very high temperatures they occur at the crossovers, so that the system is able to follow the lowest energy path highlighted in Fig. 5. At intermediate temperatures, the system shows an intermediate behavior; it does not jump at the crossovers, but it is able to undergo structural transformations well before the zero temperature jump points. The overall internal stress of the system is then reduced, and the sliding takes place more easily. The same qualitative picture will also apply, for a fixed temperature, in the case of high, low, and intermediate sliding velocities.

We thank Dr. A. P. Sutton (Department of Materials, Oxford University) for helpful discussions. C. M. acknowledges the support of the EC Human Capital and Mobility programme (Contract No. ERBCHBICT941123). The work was assisted by the HCM Network “Ab initio (from electronic structure) calculation of complex processes in materials” (Contract No. ERBCHRXCT930369).

* * *

[1] A. P. Sutton and R. W. Balluffi, *Interfaces in crystalline materials* (Oxford University Press, New York, 1995).
[2] M. C. Payne, P. D. Bristowe, and J. D. Joannopoulos,Phys. Rev. Lett. **58**, 1348 (1987).
[3] E. Tarnow, P. D. Bristowe, J. D. Joannopoulos, and M. C. Payne, J. Phys. Condens. Matter **1**, 327 (1989).
[4] E. Tarnow, P. Dallot, P. D. Bristowe, J. D. Joannopoulos, G. P. Francis, and M. C. Payne, Phys. Rev. B **42**, 3644 (1990).
[5] W. Bollmann, *Crystal Defects and Crystalline Interfaces* (Springer, Berlin, 1970).
[6] M. D. Vaudin, P. A. Lamarre, F. Schmuckle, and S. L. Sass,Philos.Mag. A **54**, 21 (1986).
[7] M. C. Payne, M. P. Teter, D. C. Allan, T. A. Arias, and J. D. Joannopoulos, Rev. Mod. Phys. **64**, 1045 (1992).
[8] P. Vogl, H. P. Hjalmarson, and J. D. Dow, J. Phys. Chem. Solids **44**, 365 (1983).
[9] G. Vogel, G. Hettich, and H. Mehrer, J. Phys. C **16**, 6197 (1983).
[10] K. C. Pandey, Phys. Rev. Lett. **57**, 2287 (1986).